Eur. Phys. J. C 4, 685–692 (1998)
DOI 10.1007/s100529800806

THE EUROPEAN PHYSICAL JOURNAL C
© Springer-Verlag 1998

The n-jet inclusive cross-section in the Hard Pomeron model

Mikhail Braun[a], Daniele Treleani

Dipartimento di Fisica Teorica dell'Università and INFN, Trieste, I-34014 Italy

Received: 29 September 1997 / Published online: 26 February 1998

Abstract. The inclusive production of several jets is studied in the framework of the hard pomeron model. The average jet momenta are found to be strongly ordered and growing towards the central c.m. rapidity, as expected. Strong positive correlations are found for pairs of jets neighbouring in rapidity, both in the forward-backward and forward-forward directions.

1 Introduction

Recent experimental data on low x behaviour of the proton structure functions at HERA [1] seem to support the idea that this behaviour is governed by an exchange of a hard ("BFKL") pomeron. However a completely inclusive character of the structure function measurements makes it very difficult to draw definite conclusions on this point. More information is likely to be obtained from less inclusive experiments in which the structure of the produced particles spectrum predicted by the hard pomeron model could be observed. In a recent publication the exclusive production rate for n jets has been calculated in this model [2]. Since it is not infrared stable, a cutoff on the lower limit of the transverse jet momentum had to be introduced. As a result, analytic calculations became impossible. Numerical results presented in [2] seem to depend crucially on the introduced infrared cutoffs both for real and virtual gluons.

In this note we draw attention to the fact that the n-jet inclusive cross-sections in the hard pomeron model admit analytic study. We calculate these cross-sections without any infrared regularization and find them infrared stable, as expected. Of course, in the infrared region the model cannot pretend to describe realistic QCD phenomena. So, to apply the model to the latter, one has to exclude this region in some way, which is important for integrated quantities, such as rapidity distributions or multiplicity moments. To this purpose introduction of some sort of cutoff is unavoidable. We however find that the model itself provides for a certain infrared regularization (although its origin is not quite conclusive, as will be discussed in the following), so that it leads to finite rapidity distributions and multilplicity moments.

Commenting on the results, we stress a characteristic dependence of the n-jet production rate on the jet transverse momenta k_i^2. Since the model is essentially logarithmic, it predicts that all $\zeta_i = \ln k_i^2$ have the order of at least $\sqrt{Y}$ where $Y = \ln s$ is the overall rapidity interval. It also predicts that all the differences $\zeta_i - \zeta_j$ have the same large order of magnitude. This means that in the model jet configurations are favoured with transverse momenta of a widely different magnitude. Due to dispesion in $\ln k^2$, the momenta of the observed jets result strongly ordered, growing from the projectile or target regions towards the center region. Also strong positive correlations are predicted both in the forward-backward and forward-forward directions. This features could be used to seek for an experimental evidence of hard pomerons.

The contents of this note is arranged as follows. In Sect. 2 we deduce a general formula for the n-jet inclusive cross-section as a function of jet rapidities and transverse momenta in the form suitable for further analytic study. In Sect. 3 we study the single and double jet inclusive cross-sections in some detail, having in mind their practical importance. Section 4 is dedicated to a discussion of higher order inclusive cross-sections, mostly in certain asymptotic regions of the phase space. Section 5 presents some conclusions.

2 The n-jet inclusive cross-sections

In the framework of the hard pomeron model jets are currently identified with emitted real gluons. The n-jet inclusive cross-section is then described by the diagram shown in Fig. 1, where also some notations for the transverse momenta and their relative energetic variables are introduced. The blobs marked G denote pomeron forward Green functions which desribe its propagation between neighbouring jets and also between the jets with a maximal or minimal rapidities and the projectile or target, respectively. The latter are characterized by their respective colour densities ρ_1 and ρ_2.

Emission of a real gluon (jet) of transverse momentum k is described by a vertex

$$\frac{12\alpha_s}{k^2} l^2 l'^2 (2\pi)^2 \delta^2(l - l' - k) \qquad (1)$$

[a] *Permanent address*: Dept. High-Energy Physics, University of St. Petersburg, 198904 St. Petersburg, Russia

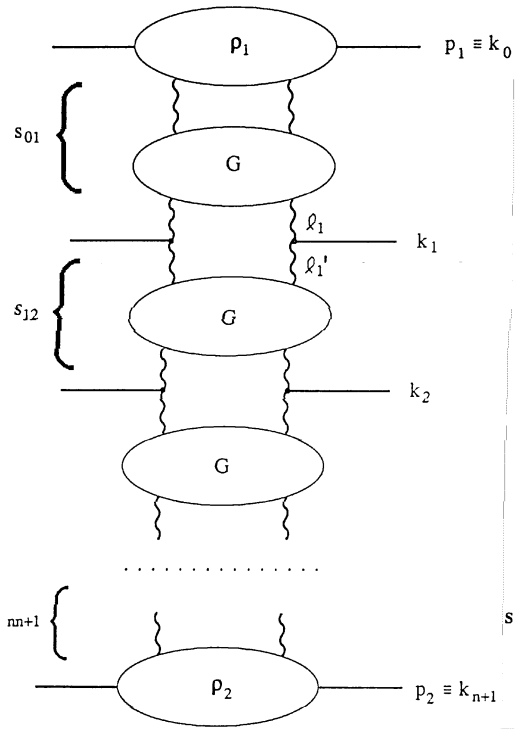

Fig. 1. The diagram which describes the n-jet inclusive cross-section

where l and l' are the reggeized gluon momenta before and after emission; α_s is the (fixed) strong coupling constant. Passing to the coordinate space, this vertex transforms into

$$\frac{12\alpha_s}{k^2}\overleftarrow{\Delta}\, e^{ikr}\overrightarrow{\Delta} \tag{2}$$

where the Laplacian operators act in the directions indicated by the arrows. Combining these vertices with the pomeron Green functions and densities ρ we obtain for the n-jet inclusive cross-section

$$\begin{aligned} I_n(y_i,k_i) \equiv \prod_{i=1}^{n}\frac{d^3}{dy_i d^2k_i}\sigma = \frac{128\pi^2}{9}\alpha_s^2\prod_{i=1}^{n}\frac{12\alpha_s}{4\pi^2k_i^2} \\ \times\int d^2r d^2r'\rho_1(r)\rho_2(r')\prod_{i=1}^{n}d^2r_i \\ \times G_{s_{01}}(r,r_1)\overleftarrow{\Delta}_1\, e^{ik_1r_1}\overrightarrow{\Delta}_1\, G_{s_{12}}(r_1,r_2) \\ \times\overleftarrow{\Delta}_2\,...\,\overrightarrow{\Delta}_n\, G_{s_{n,n+1}}(r_n,r') \end{aligned} \tag{3}$$

Here $s_{i,i+1}$ denotes the energetic variable for the pomeron between the i-th and $i+1$-th jets. In terms of jet rapidities y_i and transverse momenta k_i

$$\begin{aligned} s_{i,i+1} = |k_i||k_{i+1}e^{y_i-y_{i+1}}, \quad i\neq 0,n, \\ s_{01} = \sqrt{s}|k_1|e^{-y_1}, \quad s_{n,n+1} = \sqrt{s}|k_n|e^{y_n} \end{aligned} \tag{4}$$

Evidently they satisfy

$$\prod_{i=0}^{n}s_{i,i+1} = s\prod_{i=1}^{n}k_i^2 \tag{5}$$

Equation (3) is valid provided all energetic variables between jets are large and all momenta squared are much smaller: $k_i^2, k_{i+1}^2 << s_{i,i+1}\to\infty$. Then we approximately have

$$\ln s_{i,i+1} = y_i - y_{i+1} \equiv y_{i,i+1} \tag{6}$$

for all $i=0,..n$, with $y_0 = -y_{n+1} = \ln\sqrt{s} = (1/2)Y$. Note however, that exponentiating (6) reproduces only the dominant factor s on the right-hand side of (5).

The BFKL pomeron forward Green function $G_s(r,r')$ is well-known [3]. In the limit $s\to\infty$ we can retain only its dominant, isotropic, part

$$G_s(r,r') = \frac{rr'}{32\pi^2}\int\frac{d\nu s^{\omega(\nu)}}{(\nu^2+1/4)^2}(\frac{r}{r'})^{-2i\nu} \tag{7}$$

Alternatively we may restrict ourselves to studying only the isotropic part of the n-jet cross-section obtained after the integration over all azimuthal angles of k_i, which results in taking only the isotropic part (7) of all Green functions. Applying the Laplacian operators we find

$$\Delta G_s(r,r') = \frac{1}{8\pi^2}\int\frac{d\nu s^{\omega(\nu)}}{(1/2+i\nu)^2}(\frac{r}{r'})^{-1-2i\nu} \tag{8}$$

and a similar formula for the Laplacian operator applied to r'. As a result

$$\overrightarrow{\Delta}\, G_s(r,r')\,\overleftarrow{\Delta'} = \frac{1}{2\pi^2rr'}\int d\nu s^{\omega(\nu)}(\frac{r}{r'})^{-2i\nu} \tag{9}$$

Putting this into (3) we additionally introduce integrations over $n+1$ variables $\nu_{i,i+1},\ i=0,...n$.

At each emission vertex we then find an integral over the transverse distance r between the gluons

$$\int d^2r r^{-2-2i\nu}e^{ikr} = \frac{\pi i}{\nu+i0}(k/2)^{2i\nu}\frac{\Gamma(1-i\nu)}{\Gamma(1+i\nu)} \tag{10}$$

where for the i-th jet $\nu=\nu_{i-1,i}-\nu_{i,i+1}$. The n-jet cross-section takes the form

$$\begin{aligned} I_n(y_i,k_i^2) \\ \equiv \prod_{i=1}^{n}\frac{d^3}{dy_i dk_i^2}\sigma = \frac{4}{9}\alpha_s^2\prod_{j=1}^{n}\frac{12i\alpha_s}{8\pi^2k_j^2} \\ \times\int d^2r d^2r'\rho_1(r)\rho_2(r')rr'\prod_{i=0}^{n}d\nu_{i,i+1}s_{i,i+1}^{\nu_{i,i+1}} \\ \times\frac{r^{-2i\nu_{01}}}{(1/2+i\nu_{01})^2}\frac{r^{+2i\nu_{n,n+1}}}{(1/2-i\nu_{n,n+1})^2} \\ \times\prod_{i=1}^{n}\frac{(k_i^2/4)^{i(\nu_{i-1,i}-\nu_{i,i+1})}}{\nu_{i-1,i}-\nu_{i,i+1}+i0}\frac{\Gamma(1-i(\nu_{i-1,i}-\nu_{i,i+1}))}{\Gamma(1+i(\nu_{i-1,i}-\nu_{i,i+1}))} \end{aligned} \tag{11}$$

Now we recall that the expression (11) is valid only for large enough relative energies $s_{i,i+1}$. The exponent $\omega(\nu)$ has a maximum at $\nu=0$:

$$\omega(\nu) = \Delta - a\nu^2 + \mathcal{O}(\nu^4) \tag{12}$$

where

$$\Delta = (12\alpha_s/\pi)\ln 2 \tag{13}$$

is the pomeron intercept and

$$a = (42\alpha_s/\pi)\zeta(3) \tag{14}$$

Evidently at large $s_{i,i+1}$ small values of all $\nu_{i,i+1}$ give the dominant contribution. Consequently we can neglect ν's in all places where it is not accompanied by some large factors. The two integrations over r and r' then give average transverse dimensions of the projectile and target

$$r_{01(02)} = \int d^2 r r \rho_{1(2)}(r) \tag{15}$$

Representing

$$\frac{k^{2i\nu}}{\nu + i0} = -i\int_{\ln k^2}^{\infty} \frac{d\alpha}{2\pi} e^{i\alpha\nu}$$

we can integrate over all ν's introducing n integrations over $\alpha_i,\ i = 1, ...n$ instead. Then we obtain for the n-jet cross-section

$$I_n(y_i, k_i^2) = \frac{64}{9}\alpha_s^2 R_1 R_2 \prod_{i=1}^{n} \frac{3\alpha_s}{4\pi^3 k_i^2} \times \left(s\prod_{i=1}^{n} k_i^2\right)^{\Delta} \left(\sqrt{\pi/a}\right)^{n+1} \prod_{i=0}^{n} y_{i,i+1}^{-1/2}\, J_n \tag{16}$$

where

$$J_n = \prod_{i=1}^{n}\int_{\zeta_i}^{\infty} d\alpha_i \exp\left(-\sum_{j=0}^{n}\frac{(\alpha_j - \alpha_{j+1})^2}{4a y_{j,j+1}}\right) \tag{17}$$

and we have used the notation

$$\zeta_i = \ln k_i^2 \tag{18}$$

and have assumed $\alpha_0 = \alpha_{n+1} = 0$

Expression (16)–(17) is still far from being explicit, since integrations over α's cannot be easily done, except for the simplest case $n = 1$. However the integrand is now a positive function well behaved at all values of α's. Therefore (16)–(17) can be conveniently used both for numerical calculations and analytic study in certain limiting regions of jet parameters. Before we pass to the latter study we want to point out some evident general features of the n-jet cross-section (16)–(17).

It is clear that its overall behaviour in s is independent of n and is the same as for the total cross-section, namely, $\sim s^{\Delta}/\sqrt{\ln s}$. Indeed the characteristic values of all α's are of the order $\sqrt{y_{i,i+1}} \sim \sqrt{\ln s}$. Therefore integrations over α's will give a factor $\sim (\ln s)^{n/2}$, which will cancel a similar factor in (16) leaving one $\sqrt{\ln s}$ in the denominator. Passing to the behaviour in k_i^2, that is, in ζ_i, we observe that at large ζ_i the exponentials in the integrand provide for a damping factor at $\zeta_i > \sqrt{Y}$. As a result all ζ's and also their differencies $|\zeta_i - \zeta j|$ have large average values of the order $\sqrt{Y}$. This leads to a distribution in k_i^2 of the form discussed in the Introduction: neighbouring jets prefer to have their transverse momenta widely different in magnitude.

Of special interest is the infrared behaviour of (16)–(17), when all $\zeta_i \to -\infty$. The integrals over α's converge to a finite value in this limit. Therefore the behaviour of the cross-section in each k_i^2 will be determined by the factor $k_i^{2\Delta}/k_i^2$. Taken at its face value, it leads to the cross-section (16) integrable at small k_i^2 and thus infrared stable. However we have to acknowledge that retaining the factor $k_i^{2\Delta}$ in our formulas is in fact beyond the accuracy adopted in the lowest order hard pomeron model, in which terms containing powers of $\alpha_s \ln k^2$ have been systematically neglected. Actually the region of small k_i^2 is not only beyond the applicability of the hard pomeron model to the realistic QCD but also beyond the validity of the model itself, since, as follows from (4), it corresponds to relative energies $s_{i,i+1}$ becoming small, when the lowest order approximation fails. For this reason the small k_i^2 region has to be excluded in any case, whether one wants to apply the model to the realistic QCD or to study the model as it stands. The factors k^{Δ} which have appeared in (16) serve precisely to this purpose: they effectively cut off the small k_i^2 region. Of course, one may alternatively use harder cutoffs, as currently applied in the hard pomeron calculations, when the integration over k^2 is simply cut off at some minimal k^2_{min}. Since the difference, if any, reflects only the unknown influence of the infrared region, in the following we shall retain the factors $k^{2\Delta}$ in (16) as a natural infrared cutoff.

Finally we note that J_n, (17), can be rewritten as

$$J_n = \prod_{i=1}^{n} c_i \int_{\zeta_i/c_i}^{\infty} d\alpha_i \exp(-\sum_{j=1}^{n}\alpha_j^2 - 2\sum_{j=1}^{n-1} b_j \alpha_j \alpha_{j+1}) \tag{19}$$

where

$$c_i = \sqrt{\frac{4a y_{i-1,i} y_{i,i+1}}{y_{i-1,i+1}}},\quad b_i = \sqrt{\frac{y_{i-1,i} y_{i+1,i+2}}{y_{i-1,i+1} y_{i,i+2}}}$$

and we have denoted $y_{i,i+2} = y_{i,i+1} + y_{i+1,i+2}$. From this expression it is clearly seen that correlations are predicted between jets neighbouring in rapidity (i.e. i and $i+1$). Their strength is determined by the value of b_j's, which depends on the rapidity distances between the correlating jets and their neighbours. Evidently the correlations are maximal if the jets are emitted at the center of the rapidity interval between their neighbours and vanish if they are emitted at its borders. One also sees that the correlations are positive if the two jets have large momenta ($\zeta_i, \zeta_{i+1} > 0$), whereas they may be both positive and negative if one or both jets have very small momenta (ζ_i or/and $\zeta_{i+1} < 0$). Study of the 2-jet correlations shows that in the latter case the correlations are neglegible.

3 Single and double inclusive cross-sections

Although single jet inclusive cross-sections have already been studied rather extensively since long ago, we found

it convenient to start with them to clearly see the effect of the natural cutoff provided by the $k^{2\Delta}$ factor in (16). With it the production rate can be written explicitlly. Earlier studies mostly used harder cutofs, like just excluding the region below some chosen minimal value k^2_{min}.

The single jet inclusive cross section, obtained from (16) for $n = 1$ can be written in terms of the error function

$$I_1(y_1, k_1^2) = \frac{3\alpha_s}{4\pi^2}\sigma k_1^{2(\Delta-1)}\left(1 - \Phi(x_1)\right) \tag{20}$$

where

$$x_1 = \zeta_1\sqrt{\frac{Y}{4ay_{01}y_{12}}} \tag{21}$$

and σ is the total cross section corresponding to a pomeron exchange, which is a common factor to all inclusive cross-sections:

$$\sigma = \frac{64}{9}\alpha_s^2 R_1 R_2 s^{\Delta}\sqrt{\frac{\pi}{aY}} \tag{22}$$

For finite k_1^2 and thus finite ζ_1, the argument x_1 is small and the behavior of I_1 in k^2 is totally determined by the factor $1/k_1^2$. At very small k_1^2 ($\zeta_1 \to -\infty$) the cross-section is cut by the factor $k_1^{2\Delta}$ at values $\zeta_1 \sim -1/\Delta$. At very large k_1^2 a cutoff is provided by the error function at $\zeta_1 \sim \sqrt{4ay_{01}y_{12}/Y}$

Integrating (20) over k_1^2 one obtains the distribution in rapidity

$$I_1(y_1) = \frac{3\alpha_s}{2\pi^2\Delta}\sigma\exp(a\Delta^2 y_{01}y_{12}/Y) \tag{23}$$

Since $y_{01}y_{12} = Y^2(\frac{1}{4} - y_1^2)$ this distribution is evidently peaked at the center rapidity.

One should note that the exponent in (23) has the order $\alpha_s^3 Y$ and thus, strictly speaking should be neglected in the lowest order approximation, in which only terms of the order $\alpha_s Y$ has been taken into account. Keeping the exponent has the same meaning as retaining the factors $k^{2\Delta}$ in the initial formulas and should be considered as a natural cutoff provided by the kinematical constraints in the theory.

To find an average value of the jet momentum at a given rapidity one has to integrate (20) with the weight ζ_1 and divide by (23). One then obtains

$$\langle\zeta_1\rangle = (1/2)a\Delta(Y - 4y_1^2/Y) \tag{24}$$

As expected from the BFKL diffusion, the average momentum grows from the edges of the rapidity interval towads the center. The characteristic order of $\zeta_1 = \ln k_1^2$ results to be $\alpha_s^2 Y$, and not $\sqrt{Y}$ as deduced from the BFKL wave function properties. This also is a consequence of retaining the $k^{2\Delta}$ factor, which evidently somewhat enhances the observed jet momentum.

Integrating (23) over all rapidity range one obtains the total multiplicity as

$$\langle n\rangle = \frac{3\alpha_s}{2\pi^2\Delta^2}\sqrt{\frac{\pi Y}{a}}\exp(a\Delta^2 Y/4)\Phi\left(\frac{1}{2}\Delta\sqrt{aY}\right) \tag{25}$$

For $\Delta\sqrt{aY} << 1$ the average multiplicity grows linearly with Y, as expected. However if one takes $Y \to \infty$ keeping Δ fixed, $\langle n\rangle$ rises as a power of energy $\sim s^{a\Delta^2/4}$.

Now we pass to the double inclusive cross-section given by (16) for $n = 2$:

$$I_2(y_1, k_1^2; y_2, k_2^2) = \frac{9\alpha_s^2}{16\pi^5 a}\sigma(k_1k_2)^{2\Delta-1}\sqrt{\frac{Y}{y_{01}y_{12}y_{23}}}J_2 \tag{26}$$

where

$$J_2 = \int_{\zeta_1}^{\infty} d\alpha_1 \int_{\zeta_2}^{\infty} d\alpha_2 \times \exp\left(-\frac{\alpha_1^2}{4ay_{01}} - \frac{(\alpha_1 - \alpha_2)^2}{4ay_{12}} - \frac{\alpha_2^2}{4ay_{23}}\right) \tag{27}$$

As seen from (19) real parameters of the integral (27) are $\zeta_1/\sqrt{4aY}$ and $\zeta_2/\sqrt{4aY}$. So for finite jet momenta one can put $\zeta_1 = \zeta_2 = 0$ and the integral, which turns out independent of jet momenta, can be easily calculated;

$$J_2 = \pi a\sqrt{y_{01}y_{12}y_{23}/Y}\left(1 + \frac{2}{\pi}\arctan\sqrt{\frac{y_{01}y_{23}}{y_{12}Y}}\right)$$

so that the inclusive cross-section becomes

$$I_2(y_1, k_1^2; y_2, k_2^2) = \frac{9\alpha_s^2}{16\pi^4}\sigma(k_1^2k_2^2)^{\Delta-1} \times \left(1 + \frac{2}{\pi}\arctan\sqrt{\frac{y_{01}y_{23}}{y_{12}Y}}\right) \tag{28}$$

For general ζ_1 and ζ_2 the integral (27), which is an evident generalization of the error function to two dimensions, cannot be done analitically and requires numerical calculation. We have calculated the ratio

$$R(y_1, k_1^2; y_2, k_2^2) = \frac{\sigma I_2(y_1, k_1^2; y_2, k_2^2)}{I_1(y_1, k_1^2)I_1(y_2, k_2^2)} \tag{29}$$

to study correlations between the emitted jets. Absence of correlations corresponds to $R = 1$. In Fig. 2 we show results of the numerical calculation of R for a symmetric pair of jets at $y_1 = -y_2 = Y/6$, which divide the rapidity interval into three equal parts. R is presented as a function of $z_2 = \zeta_2/\sqrt{4aY}$ in the interval $0 \le z_2 \le 2$ for fixed values of $z_1 = \zeta_1/\sqrt{4aY} = 0, 1, 2$. For negative ζ_1 or/and ζ_2 we find that $R = 1$ and there are no correlations. One observes from Fig. 2 that there are significant positive correlations between the two jets in the whole region of positive ζ_1 and ζ_2 corresponding to momenta which are not small relative to the intrinsic scale of the BFKL model (which should be supplied by higher orders of the theory). They should be seen experimentally as positive forward-backward correlations in the c.m. system.

For very large jet momenta, when ζ_1 or/and ζ_2 become of the order $\sqrt{4aY}$, the correlations become very strong and grow very fast with ζ's, reaching values of the order $4.\,10^5$ at $\zeta_1 = \zeta_2 = 2$. However one should have in mind that at such high momenta the production rate gets exceedingly small, beyond any possibility of experimental

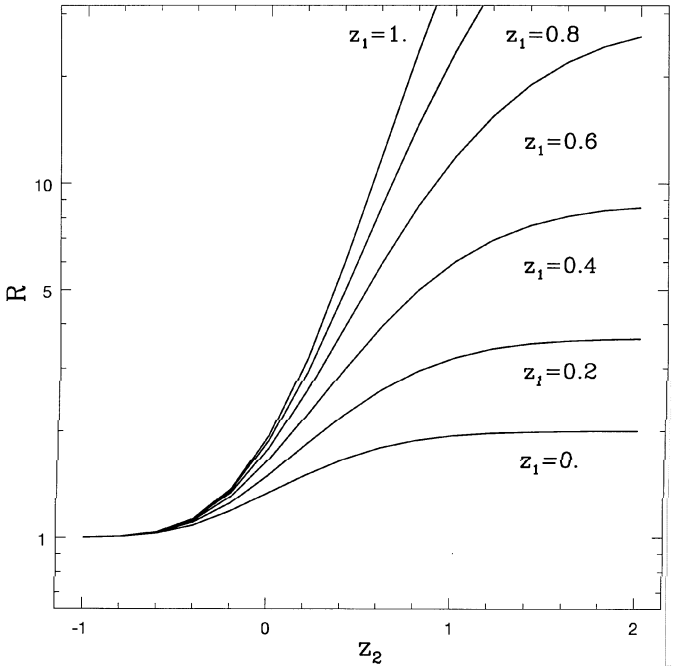

Fig. 2. The ratio R (29) for two jets with $y_1 = -y_2 = Y/3$ as a function of $z_2 = \ln k_2^2/\sqrt{4aY}$ for different values of $z_1 = \ln k_1^2/\sqrt{4aY}$

detection, which can be deduced from (20), so that such high values of R bear, in fact, no physical importance.

We have also calculated the ratio R for two jets emitted both in the forward hemisphere, with $y_1 = Y/3$ and $y_2 = Y/6$. The results are quite similar qualitatively, although the numerical values result a bit different (however of the same order of magnitude). Thus one should also expect forward-forward correlations of the same order as the forward-backward ones.

Integrating (26) over the two momenta k_1^2 and k_2^2 one obtains the double distribution in rapidity. These integrations can easily be done explicitly using an evident formula

$$\int_{-\infty}^{+\infty} d\zeta e^{\Delta\zeta} \int_{\zeta}^{+\infty} d\alpha f(\alpha) = (1/\Delta) \int_{-\infty}^{+\infty} d\zeta e^{\Delta\zeta} f(\zeta) \tag{30}$$

valid for any $f(\alpha)$ integrable at $\alpha = \pm\infty$. We obtain

$$I_2(y_1, y_2) = \left(\frac{3\alpha_s}{2\pi^2\Delta}\right)^2 \sigma \exp \times \left(a\Delta^2(y_{01} + y_{23} - (y_{01} - y_{23})^2/Y)\right) \tag{31}$$

The exponential factor again comes from the kinematical factor $k^{2\Delta}$ and has a higher order than normally taken into account in the BFKL theory. If we neglect it, we obtain a completely flat distribution in the two rapidities. The exponential factor evidently has its maximum when the two jets are both emitted at central rapidity $y_1 = y_2 = 0$, when it grows like $\exp(a\Delta^2 Y)$. Comparing to (23) we observe that it also introduces positive correlations between the two jets in the rapidity space. In fact, the ratio analogous to (29) results

$$R(y_1, y_2) = \frac{\sigma I_2(y_1, y_2)}{I_1(y_1) I_1(y_2)} = \exp(a\Delta^2 y_{01} y_{23}/Y) \tag{32}$$

and evidently implies positive correlations, growing as the two jets move to the central rapidity region.

Integrating (31) over all the rapidity region we obtain the second moment of the distribution in the numer of jets. Neglecting the exponential factor we get

$$\langle n(n-1)\rangle = \left(\frac{3\alpha_s}{2\pi^2\Delta}\right)^2 Y^2 = \langle n\rangle^2 \tag{33}$$

With the exponential factor taken into account, the second moment can be found only by numerical integration.

4 Multijet inclusive cros-sections

The features found for the production of two jets repeat themselves in the multijet production. However for $n > 2$ analytic results cannot be obtained for most of the observables. So one can only study cases corresponding to some limiting parts of the phase space.

4.1 Distributions in rapidities and momenta

As mentioned the real parameters of the cross-section are ratios $\zeta_i/\sqrt{4aY}$. Depending on their values we may distinguish between three asymptotic regions, in which the cross-section (16) can be estimated by standard asymptotic methods.

The first region is the infrared one, when $\zeta_i \to -\infty$ faster than $\sqrt{Y} \to \infty$. In this region the cross-section is given by (16) with the integrals J_n independent of k_i^2 and given by

$$J_n = \prod_{i=1}^{n} \int_{-\infty}^{\infty} d\alpha_i \exp\left(-\sum_{j=0}^{n} \frac{(\alpha_j - \alpha_{j+1})^2}{4ay_{j,j+1}}\right) \tag{34}$$

To do this integral we pass to variables

$$\alpha_{i,i+1} = \alpha_i - \alpha_{i+1}, \quad i = 0, ...n \tag{35}$$

subject to condition $\sum_{i=0}^{n} \alpha_{i,i+1} = 0$ and present

$$J_n = \int_{-\infty}^{\infty} \frac{d\lambda}{2\pi} \prod_{i=0}^{n} \int_{-\infty}^{\infty} d\alpha_{i,i+1} \exp \sum_{j=0}^{n} \left(i\lambda - \frac{\alpha_{j,j+1}^2}{4ay_{j,j+1}}\right) \tag{36}$$

All integrals are trivial and we get

$$J_n = \frac{1}{2\pi}\sqrt{\frac{\pi}{aY}} \prod_{i=0}^{n} (4\pi a y_{i,i+1})^{1/2} \tag{37}$$

Thus in the infrared region we have the cross-section

$$I_n(y_i, k_i^2) = (\frac{3\alpha_s}{2\pi^2})^n \sigma (\prod_{i=1}^{n} k_i^2)^{\Delta-1} \tag{38}$$

As one observes, the infrared cross-section is independent of individual jet rapidities: the distribution in all y_i is completely flat. The dependence on k_i^2 apart from the canonical factor $1/k_i^2$ exhibits an extra factor discussed above $k_i^{2\Delta}$, which serves as an effective infrared cutoff.

The second region is that of low k_i^2, when ζ_i are finite and thus all ratios $\zeta/\sqrt{Y}$ go to zero. In this region the inclusive cross-section is given by (16) with the integral J_n again independent of k_i^2:

$$J_n = \prod_{i=1}^{n} \int_0^\infty d\alpha_i \exp\left(-\sum_{j=0}^{n} \frac{(\alpha_j - \alpha_{j+1})^2}{4a y_{j,j+1}} \right) \tag{39}$$

The dependence on k_i^2 is thus the same as in the infrared region. However there appears now a nontrivial dependence on rapidities.

The integral (39) can be easily done only for $n = 1, 2$ (see Sect. 3). Calculation of J_n for larger n can be done by numerical methods. Analytic estimate of J_n is possible within the saddle point method, presumably valid for large n. Denote

$$P = \sum_{i=0}^{n} \frac{(\alpha_i - \alpha_{i+1})^2}{4a y_{i,i+1}} \equiv \sum_{i=0}^{n} b_{i,i+1} (\alpha_i - \alpha_{i+1})^2 \tag{40}$$

We have

$$\sum_{i=k+1}^{k+m} \partial P/\partial \alpha_i = 2b_{k,k+1}(\alpha_{k+1} - \alpha_k) + 2b_{k+m,k+m+1}(\alpha_{k+m} - \alpha_{k+m+1}) \tag{41}$$

If we require that

$$\partial P/\partial \alpha_i = 0, \tag{42}$$

for all $i = 1, ...n$ then, recalling that $\alpha_0 = \alpha_{n+1} = 0$, we shall obtain an homogeneous system of linear equations in $\alpha_i, i = 1, ...n$ with a nonsingular matrix, so that the solution will be that all α are zero, i.e. at the initial integration point. Thus there are no saddle points inside the overall integration volume in all α's. We can, however, relax condition (42), by fixing one of the α's, say α_n, thus seeking a saddle point on the surface, inside the integration volume in all other α_i, $i = 1, ...n-1$. Putting $k + m = n - 1$ in (41), we get

$$\alpha_k - \alpha_{k+1} = -\frac{b_{n-1,n}}{b_{k,k+1}} (\alpha_{n-1} - \alpha_n) \tag{43}$$

Summing these equations for $k = 0, ..j - 1$ we obtain

$$-\alpha_j = b_{n-1,n}(\alpha_{n-1} - \alpha_n) \sum_{k=0}^{j-1} 1/b_{k,k+1} \equiv \frac{b_{n-1,n}}{b_{0j}} (\alpha_{n-1} - \alpha_n) \tag{44}$$

Here and in the following we use the notation

$$1/b_{j,j+m} = \sum_{k=j}^{j+m-1} 1/b_{k,k+1} = 4a(y_j - y_{j+m}) \tag{45}$$

Putting $j = n$ in (44), we can express the difference $\alpha_{n-1} - \alpha_n$ in terms of the fixed variable α_n. Combining this with (44) we finally find

$$\alpha_j = \frac{b_{0,n}}{b_{0,j}} \alpha_n \tag{46}$$

Equation (46) determine the position of the saddle point in α_i, $i = 1, ...n-1$ in terms of the fixed α_n. At the saddle point we find

$$P = \sum_{i=0}^{n-1} b_{i,i+1} \left(\frac{b_{n-1,n}}{b_{i,i+1}} (\alpha_{n-1} - \alpha_n) \right)^2 + b_{n,n+1}\alpha_n^2 = \alpha_n^2 (b_{0n} + b_{n,n+1}). \tag{47}$$

Integration over the saddle point gives a factor

$$\sqrt{\frac{\pi^{n-1}}{\det M}}$$

where M is an $(n-1)\times(n-1)$ matrix of second derivatives. Simple calculations give

$$\det M = (1/b_{0,n}) \prod_{i=0,n-1} b_{i,i+1} \tag{48}$$

The integration over α_n adds a factor $\frac{1}{2}\sqrt{\pi/(b_{0n} + b_{n,n+1})}$. and we get the contribution from the surface $\alpha_n = 0$

$$J_n = \frac{1}{4\pi} \sqrt{\frac{\pi}{aY}} \prod_{i=0}^{n} (4\pi a y_{i,i+1})^{1/2} \tag{49}$$

which is one half of (37). Taking into account all other surface contributions will multiply (49) by n. As a result, we obtain for the inclusive cross-section an expression which is identical to (38) except for an extra factor $n/2$. The distribution in rapidities obtained by this asymptotic estimate is again completely flat.

We finally pass to the third asymptotic region, that of high k_i^2, which corresponds to all $\zeta_i/\sqrt{y} \to \infty$. In this region the behaviour of the integral (17) is governed by the damping exponentials in the integrand. To find the asymptotics we may again recur to the saddle point method. However in this region the integration volume depends on the values of ζ_i and we have to check whether the found saddle point lies inside this volume. As a result, the set of α's for which the saddle point lies inside the integration volume will depend on the values of ζ_i and will generally be only a part of all α's. The rest of α's will be restricted to their initial values ζ's, since in absence of a saddle point the integrand falls with each α exponentially. The asymptotics will thus depend in a rather complicated way on the manner in which different ζ's get large and also on the jet rapidities. Nevertheless it is not difficult to find this asymptotics for given y_i and large ζ_i.

Let us consider a situation when a particular set of α's take on their initial values in the asymptotics, the rest of them integrated over their saddle points. Take a pair of jets, the j th and $(j + m)$th, for which α's take on their

initial values with all intermediate jets from $(j+1)$th to $(j+m-1)$th having a saddle point inside the integration volume. In other words (42) are satisfied for $i = j+1, ...j+m-1$ with $\alpha_j = \zeta_j$ and $\alpha_{j+m} = \zeta_{j+m}$. Repeating the procedure described above we can solve these equations for the saddle point $\alpha_i, i = j+1, ...j+m-1$ in terms of ζ_j and ζ_{j+m-1}. We find

$$\alpha_{j+k} = \zeta_j + \frac{b_{j,j+m}}{b_{j,j+k}}(\zeta_{j+m} - \zeta_j) > \zeta_{j+k}, \quad k = 1, ...m-1 \tag{50}$$

The last inequality follows from the condition that the saddle point should lie inside the integration volume. This inequality determines a certain domain in the jet phase space y_i, k_i^2 where this particular type of asymptotic behaviour will take place. The part of the exponential P containing α's from the $(j+1)$th to $(j+m-1)$th, at the saddle point becomes equal to

$$b_{j,j+m}(\alpha_j - \alpha_{j+m})^2$$

that is, takes the same form as if there were no other jets between the j th and $(j+m)$ th ones. Integration over all $\alpha_i,\ i = j+1, ...j+m-1$ by the saddle point method thus gives a factor

$$\sqrt{\frac{\pi^{m-1} b_{j,j+m}}{\prod_{i=j}^{j+m-1} b_{i,i+1}}} \tag{51}$$

and leaves an integrand where these jets have disappeared. Doing this with all sets of α's which have their saddle point inside the integration volume we shall obtain more factors (51) and an integral over remaining α's in which all other jets have disappeared and which does not contain saddle points inside the integration volume. Integrating by parts one obtains for the latter integral an asymptotics

$$\frac{1}{\prod \partial P/\partial \alpha_i}_{\alpha_i = \zeta_i} \exp\left(-\sum_{i<k} b_{i,k}(\zeta_i - \zeta_k)^2\right) \tag{52}$$

Both the product and sum go over the jets remaining after exclusion of the ones integrated over their saddle points. The described asymptotics will evidently be valid in the domain where the inequality (50) is fulfilled for these excluded jets.

To make this rather complicated prescription more understandable, consider a simple case when rapidity distances between neighbouring jets are all equal: $y_{i,i+1} = \Delta y$ independent of i. Then the left hand side of inequality (50) represents a direct line in the i, ζ plane connecting points ζ_j and ζ_{j+m}. The inequality (50) means that the intermediate $\zeta_i,\ i = j+1, ...j+m-1$ lie below this line. The prescription for the asymptotics is then to draw all lines connecting given $\zeta_i,\ i = 0, 1, ..n, n+1$, where by definition $\zeta_0 = \zeta_{n+1} = 0$. If some ζ's happen to lie below any such line, one should throw the corresponding jets out introducing factors (51) instead. In the end only ζ's will remain which lie above any line connecting a pair of them, that is the remaining ζ_i will represent a convex line in the i, ζ plane. The behaviour in these ζ's will be described by (52). Of course, if if all ζ_i form a convex line from the start, the asymptotics will have the form (52) with a product and sum going over all $i = 1, ...n$.

For illustration consider a case $n = 2$. Condition that points $\zeta_0 = 0, \zeta_1, \zeta_2, \zeta_3 = 0$ form a convex function of i is evidently

$$|\zeta_1 - \zeta_2| < \zeta_1,\ \zeta_2 \tag{53}$$

In this region the asymptotics will be

$$I_2 = \frac{3\sqrt{3}\alpha_s^2}{4\pi^5} aY\sigma(k_1^2 k_2^2)^{\Delta-1} \frac{1}{\zeta_1\zeta_2 - 2(\zeta_1 - \zeta_2)^2} \times \exp\left(-\frac{\zeta_1^2 + \zeta_2^2 + (\zeta_1 - \zeta_2)^2}{(4/3)aY}\right) \tag{54}$$

Now take the region

$$2\zeta_1 < \zeta^2 \tag{55}$$

where ζ_1 lies below the line connecting $\zeta_0 = 0$ and ζ_2. According to our prescription the first jet now gives a factor (51) and the second gives (52). We thus obtain

$$I_2 = \frac{27\sqrt{2}\alpha_s^2}{8\pi^4}\sqrt{\frac{aY}{\pi}}\sigma(k_1^2 k_2^2)^{\Delta-1}\frac{1}{\zeta_2}\exp\left(-\frac{\zeta_2^2}{4aY}\right) \tag{56}$$

In the symmetric region $2\zeta_2 < \zeta_1$ we shall evidently obtain (56) with the first and second jets interchanged.

4.2 Integrated distributions

Integrating (16) over all k_i^2 we get rapidity distributions $I_n(y_i)$. As discussed, these integrations converge in the infrared region due to the cutoff factors $k_i^{2\Delta}$. Using (30) we obtain from (16)

$$I_n(y_i) = (\frac{3\alpha_s}{4\pi^2\Delta})^n (\sqrt{\frac{\pi}{a}})^n \sigma\sqrt{Y}\prod_{i=0}^{n} y_{i,i+1}^{-1/2}\, K_n \tag{57}$$

where

$$K_n = \int_{-\infty}^{+\infty}\prod_{i=1}^{n} d\zeta_i \exp \times\left(\Delta\sum_{i=1}^{n}\zeta_i - \sum_{i=0}^{n} b_{i,i+1}(\zeta_i - \zeta_{i+1})^2\right) \tag{58}$$

and $\zeta_0 = \zeta_{n+1} = 0$ and $b_{i,i+1}$ are defined by (40). The integral (58) can be easily calculated using the same technique that was applied to obtain (37). In terms of variables $\zeta_{i,i+1} = \zeta_i - \zeta_{i+1}$, the sum of which is zero, we find

$$\sum_{i=1}^{n}\zeta_i = (1/2)\sum_{i=0}^{n}(n-2i)\zeta_{i,i+1} \tag{59}$$

The integral K_n becomes

$$K_n = \int_{-\infty}^{+\infty} \frac{d\lambda}{2\pi} \prod_{i=1} n d\zeta_i \exp \sum_{i=0}^{n} \big((i\lambda + (n/2 - i)\Delta) \times \zeta_{i,i+1} - b_{i,i+1}(\zeta_i - \zeta_{i+1})^2 \big)$$
$$= \frac{1}{2\pi} \prod_{i=0}^{n} (4\pi a y_{i,i+1})^{1/2} \times \exp\left(\frac{a\Delta^2}{4Y} (n^2 Y^2 + 8\rho Y - 4(n+1)\sigma Y - 4\sigma^2) \right) \quad (60)$$

where

$$\sigma = \sum_{k=1}^{n} y_k, \quad \rho = \sum_{k=1}^{n} k y_k \quad (61)$$

Putting (60) into (57) we obtain finally

$$I_n(y_i) = (\frac{3\alpha_s}{2\pi^2 \Delta})^n \sigma \times \exp\left(\frac{a\Delta^2}{4Y} (n^2 Y^2 + 8\rho Y - 4(n+1)\sigma Y - 4\sigma^2) \right) \quad (62)$$

As in the two-jet case, the exponential factor lies, in fact, outside the precision, normally adopted in the lowest order BFKL model. If we neglect it we evidently obtain a completely flat distribution in all rapidities. The effect of the exponential factor can easily be seen. Let $\phi = n^2 Y^2 + 8\rho Y - 4(n+1)\sigma Y - 4\sigma^2$. Since the derivatives $\partial\phi/\partial y_k = Y(8k - 4(n+1)) - 8\sigma,\ k = 1, ...n$ cannot all be equal to zero simultaneously, the maximum of ϕ occurs at limiting values of its arguments, that is, when all y_i coincide: $y_1 = y_2 = ... = y_n$. At this point $\phi = n^2(Y^2 - 4y_1^2)$. The maximum is achieved at $y_1 = 0$ and is equal to $n^2 Y^2$. Thus the exponential factor favours emission of all jets at central rapidity transforming a flat plateau into a convex one.

Integration of $I(y_i)$ over all y_i gives multiplicity moments. With a flat distribution we immediately get

$$\langle n(n-1)...(n-k+1) \rangle = (\frac{3\alpha_s}{2\pi^2 \Delta})^k Y^k = \langle n \rangle^k \quad (63)$$

This corresponds to a Poissonian distribution in n, with the average $\langle n \rangle$ growing like Y, in confirmation of simple estimates. The exponential factor in (62) will, in all probability, make the moments grow more rapidly, like powers of energy, as follows from the case $n = 1$ studied in Sect. 3

5 Conclusions

We have studied inclusive production of many jets in the hard pomeron model, with a special emphasis on the two-jet production. In confirmation of current expectations, we found that the average jet momenta are strongly ordered, monotonously growing from the projectile or target regions to the central regions. The most characteristic feature of multiple jet production seems to be strong positive correlations between jets neigbouring in rapidity, both in the forward-backward and forward-forward directions.

In our treatment we have preserved kinematical factors $k^{2\Delta}$, which serve as a natural infrared cutoff and allow to obtain finite analytic expressions for distributions in rapidity and number of jets. As a consequence we also obtained an enhancement in the high k^2 region, so that the average values $\langle \ln k^2 \rangle$ result growing like $\alpha_s^2 Y$ and not like $\sqrt{\alpha_s Y}$ as concluded from the study of the pomeron wave function. To see the relevance of this effect, one has to study the second order corrections in the hard pomeron model, which now seems possible, but lies beyond the scope of the present study.

Acknowledgements. M.A. Braun thanks the INFN and the University of Trieste for their financial help during his stay at Trieste.

References

1. ZEUS Collaboration. M.Derrick et al., Z.Phys. **C69** (1996) 607;
   H1 Collaboration. T. Ahmed et al., Nucl. Phys., **B439** (1995) 471
2. J. Kwiecinski, A.D. Martin, R.G. Roberts, Phys. Rev. D
3. L.N. Lipatov, in: "Perturbative QCD", ed. by A.H. Mueller, World Scientific, Singapore (1989)